Developmental Biology 447 (2019) 170–181

Contents lists available at ScienceDirect

Developmental Biology

journal homepage: www.elsevier.com/locate/developmentalbiology

Original research article

The cadherin-catenin complex is necessary for cell adhesion and embryogenesis in *Nematostella vectensis*

D. Nathaniel Clarke[a,*], Christopher J. Lowe[a,*], W. James Nelson[a,b]

[a] Department of Biology, Stanford University, Stanford CA 94305, United States
[b] Department of Molecular and Cellular Physiology, Stanford University, Stanford CA 94305, United States

ARTICLE INFO

Keywords:
Cnidaria
Nematostella
Calcium
Adhesion
Cadherin
Catenin

ABSTRACT

The cadherin-catenin complex is a conserved, calcium-dependent cell-cell adhesion module that is necessary for normal development and the maintenance of tissue integrity in bilaterian animals. Despite longstanding evidence of a deep ancestry of calcium-dependent cell adhesion in animals, the requirement of the cadherin-catenin complex to coordinate cell-cell adhesion has not been tested directly in a non-bilaterian organism. Here, we provide the first analysis of classical cadherins and catenins in the Starlet Sea Anemone, *Nematostella vectensis*. Gene expression, protein localization, siRNA-mediated knockdown of α-catenin, and calcium-dependent cell aggregation assays provide evidence that a *bonafide* cadherin-catenin complex is present in the early embryo, and that α-catenin is required for normal embryonic development and the formation of cell-cell adhesions between cells dissociated from whole embryos. Together these results support the hypothesis that the cadherin-catenin complex was likely a complete and functional cell-cell adhesion module in the last common cnidarian-bilaterian ancestor.

Summary statement: Embryonic manipulations and *ex vivo* adhesion assays in the sea anemone, *Nematostella vectensis*, indicate that the necessity of the cadherin-catenin complex for mediating cell-cell adhesion is deeply conserved in animal evolution.

1. Introduction

The evolution of cell-cell adhesion mechanisms has long been associated with the development of complex multicellular organisms (Abedin and King, 2010; Grosberg and Strathmann, 2007; Knoll, 2011). Early investigators interested in the origins of metazoans (multicellular animals) first studied the aggregation of the dissociated cells of sponges as a means of exploring how cell adhesion contributes to tissue organization and self- / non-self-identity (Wilson, 1907). From these initial investigations, hints of the molecular basis of animal cell adhesion emerged, as it was discovered that cell-cell adhesion was dependent on the presence of calcium in a diversity of organisms from sponges to sea urchins (Herbst, 1900; Maas, 1906). This property of calcium-dependence led to the discovery of the cadherin trans-membrane protein family in tissue culture cells (Takeichi, 1977), which, together with their key intracellular binding partners the catenins, constitute a protein complex (the cadherin-catenin complex; CCC) that is essential for cell adhesion in complex bilaterian animals (Halbleib and Nelson, 2006; Miller et al., 2012; Takeichi, 1988).

The CCC mediates cell adhesion in tissues by coupling neighboring cells at the Adherens Junction (AJ), and is required for normal development and the maintenance of organized adult tissues in complex animals (Fig. 1A) (Gumbiner, 2005; Harris and Tepass, 2010; Larue et al., 1996; Nelson, 2008). A fundamental tissue building block of all animal body plans is a simple epithelium, which compartmentalizes specialized internal conditions from the external environment (Cereijido et al., 2004; Miller et al., 2012). The CCC creates a mechanical connection between epithelial cells by linking classical cadherin adhesion proteins to the actin cytoskeleton (Borghi et al., 2012). In the presence of calcium, the calcium-dependent adhesion domains (CADs) of opposing cadherins become structurally rigid and interact with each other in the extracellular space (Nagar et al., 1996). In the cytoplasm, cadherins bind to β-catenin through a conserved motif in the unstructured cytoplasmic tail. β-Catenin in turn binds to α-catenin, a filamentous (F-) actin-binding protein that links cadherin adhesions to the cytoskeleton at the AJ (Fig. 1A)(Aberle et al., 1996; Buckley et al., 2014). Mutations in the CCC produce catastrophic developmental defects that manifest as failures in gastrulation and morphogenesis in the early embryo, and in most cases result in

* Corresponding authors.
E-mail addresses: clarken@stanford.edu (D. Nathaniel Clarke), clowe@stanford.edu (C.J. Lowe), wjnelson@stanford.edu (W. James Nelson).

https://doi.org/10.1016/j.ydbio.2019.01.007
Received 20 July 2018; Received in revised form 20 December 2018; Accepted 4 January 2019
Available online 07 January 2019
0012-1606/

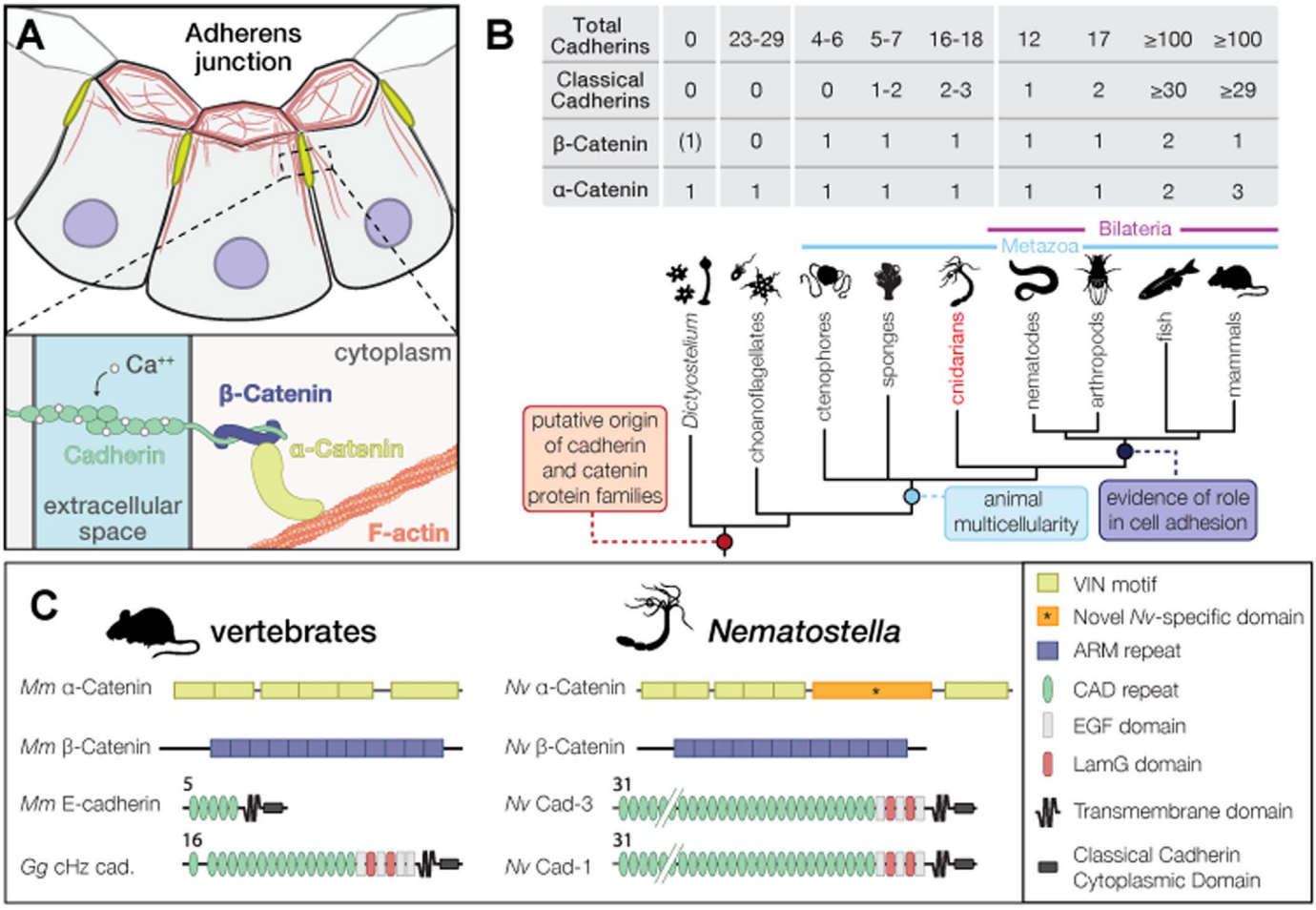

Fig. 1. Cadherin/Catenin proteins in the genome of *N. vectensis* versus other animals. A. (top) schematic representation of the adherens junction (yellow) linking the cortical actomyosin network (red) between neighboring cells; (bottom) illustration of the cadherin-catenin complex within the adherens junction, with calcium-dependent interactions between cadherins (green), are linked by β- (blue) and α-Catenin (yellow) to F-Actin (red). B. The presence, absence, and abundance of cadherin/catenin components across animal lineages and non-animal relatives, with a phylogenetic tree for reference. C. The cadherin-catenin complement from *N. vectensis* in comparison to representative vertebrate orthologs. (For interpretation of the references to color in this figure legend, the reader is referred to the web version of this article.)

developmental arrest (Costa et al., 1998; Kane et al., 1996; Larue et al., 1996, 1994; Stepniak et al., 2009; Torres et al., 1997).

Due to its crucial role in bilaterian model organisms, cell-cell adhesion mediated by the CCC has been proposed to be a fundamental ancestral innovation in metazoans coincident with the evolution of multicellularity. Genes encoding core components of the CCC are present in the genomes of all sequenced metazoan phyla, and are partly or wholly absent from the genomes of closely related non-metazoan lineages (Fig. 1B) (Abedin and King, 2008; Hulpiau and van Roy, 2011; Miller et al., 2012; Nichols et al., 2006, 2012). However bioinformatics studies have demonstrated that the components of the complex have a deep ancestry that far predates animal multicellularity (Miller et al., 2012), and have cast doubt on whether the CCCs of basally branching animal phyla are likely to function in epithelial cell-cell adhesion (Belahbib et al., 2018).

Experimental evidence suggests that the CCC arose from two independent modules, an extracellular cadherin adhesion module and a cytoplasmic catenin and actin-binding module, that were co-opted into a single functional complex at some point in early animal evolution (Miller et al., 2012). The slime mold *Dictyostelium*, a distant animal relative, lacks cadherins entirely, but has an α-catenin/β-catenin actin-binding module that is necessary to organize an epithelia-like structure (the fruiting body) during its multicellular life history stage (Dickinson et al., 2011). Choanoflagellates, which are the eukaryotic sister group of metazoans, have cadherin-like proteins which contain CAD domains, but lack classical cadherin catenin-binding motifs, and their genomes entirely lack a β-catenin ortholog: instead, choanoflagellates rely on C-type lectin-like proteins and cell-extracellular matrix (ECM) adhesion to join daughter cells of incomplete mitoses together in a limited multicellular development (Abedin and King, 2008; Dayel et al., 2011; Fairclough et al., 2010; Levin et al., 2014). Sponges (Porifera), one of the earliest animal lineages, have a full set of CCC genes (Srivastava et al., 2010) and some descriptive evidence suggests that CCC components localize to cell junctions (Miller et al., 2018; Nichols et al., 2012; Schippers and Nichols, 2018), but experimental evidence also indicates that secreted glycoprotein 'Aggregation Factors' and ECM may be responsible for organizing sponge cell-cell adhesion (Misevic and Burger, 1993; Varner, 1995), and there is currently no direct experimental evidence suggesting that the CCC is necessary for adhesion in sponge tissues.

While the necessity for the CCC in coordinating cell adhesion in a non-bilaterian animal has not been demonstrated, recent evidence from *in vitro* biochemical studies of the CCC in the cnidarian sea anemone, *Nematostella vectensis*, has suggested that its core functions are conserved across all eumetazoans (cnidarians and bilaterians) (Clarke et al., 2016). *N. vectensis* has a complete set of CCC proteins: its genome encodes two exceptionally long classical cadherins, Cadherin 1 and Cadherin 3, each of which possesses 31 extracellular cadherin repeats (Pukhylakova et al., pers. communication; see acknowledgements), and a single ortholog of β-catenin and α-catenin (Hulpiau and van Roy, 2011) (Fig. 1C). Despite moderate sequence dissimilarities to their vertebrate orthologs, these proteins form a

ternary complex with a 1:1:1 stoichiometry similar to their vertebrate counterparts (Clarke et al., 2016). This suggests that the CCC could be a functional adhesion module in *N. vectensis*, but this hypothesis remains to be tested in the organism.

Here, we provide the first analysis of classical cadherins, and α- and β-catenin during early development of *N. vectensis*, as well as insight into their necessity for cell adhesion during development through functional perturbation of α-catenin. Together, gene expression, protein localization, siRNA-mediated knockdown of α-catenin, and calcium-dependent cell aggregation assays provide novel evidence supporting the presence of a *bonafide* CCC in early embryonic development in *N. vectensis*.

2. Results

2.1. α-Catenin, β-catenin, and Cadherin 3 are expressed ubiquitously in the early embryo

We examined the expression and localization of Cadherin (Cad.) 1 and 3, and α- and β-catenin from early cleavage through mid-larval

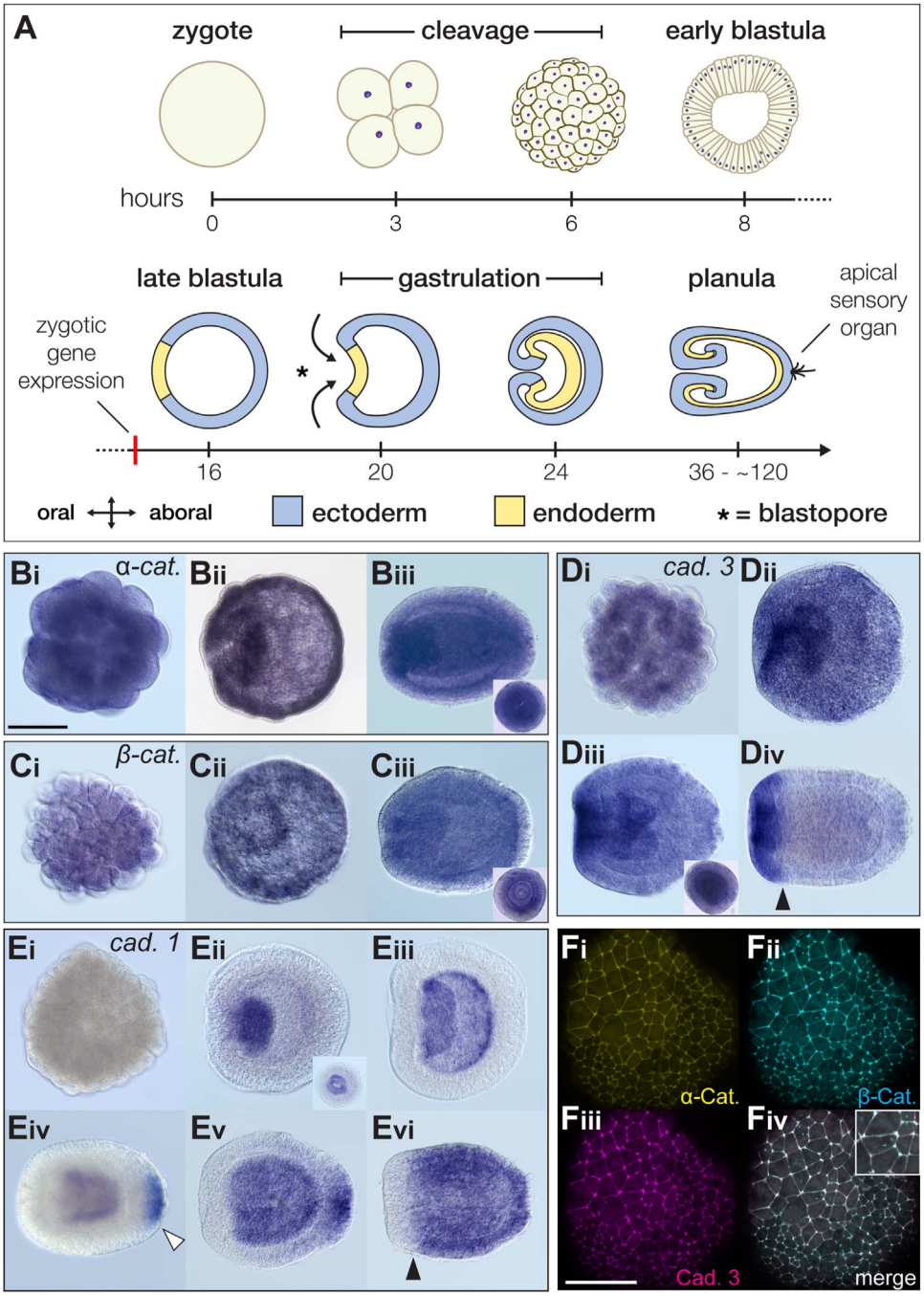

Fig. 2. *N. vectensis* α-catenin, β-catenin, and Cadherin 3 are co-expressed in the early embryo and localize to apical cell junctions. A. Schematic of normal development in *N. vectensis*; arrows indicate invagination movements at the onset of gastrulation, asterisk indicates the blastopore, and red line indicates the timing of zygotic gene expression. Whole-mount *in situ* hybridization of *α-catenin* Bi - Biii), *β-catenin* (Ci - Ciii), *cadherin 3* (Di - Div), and *cadherin 1* (Ei - Evi) from early embryonic through mid-larval stages. Insets in Biii, Ciii, and Diii are blastoporal views of embryos bisected with the blade of a 22-gauge syringe to show internal staining; inset in Eii is a blastoporal view of a whole gastrula-stage embryo. Fi-iv. confocal maximum projection of a 6-h blastula embryo co-injected with fluorescent fusion mRNAs encoding α-catenin: mNeonGreen (Fi), β-catenin: mTagBFP2(Fii), and Cadherin 1: mScarlet (Fiii); images are of a single embryo, but representative of 3 separate experiments of 20 or more embryos each. Scale bars are 50 μm throughout.

stages in the embryo using whole-mount in situ hybridization; hybridizations with anti-sense probes (Fig. 2) were compared to sense probes as a negative control (Supp. Fig. 1). During development, the first epithelial tissue forms in the early blastula stage embryo, following multiple rounds of synchronous cell divisions during cleavage stages (Fig. 2A) (Fritzenwanker et al., 2007). Zygotic gene expression begins during the blastula stage prior to the onset of gastrulation, and thus it can be inferred that transcripts detected in earlier stages are likely maternally provisioned (Helm et al., 2013). Gastrulation via invagination follows, along with the establishment of the endoderm, and these cell movements and fate specifications comprise the major morphogenetic and transcriptional events during early embryogenesis (Fig. 2A) (Magie et al., 2007; Röttinger et al., 2012).

In situ hybridization showed that mRNAs encoding α- and β-catenin are co-expressed ubiquitously at all observed stages (Fig. 2Bi-iii, Ci-iii). Cad. 3 mRNA is also expressed ubiquitously in a similar manner, with the notable difference of higher levels of expression in the blastopore lip and pharyngeal ectoderm in the early planula stage compared to the catenins (Fig. 2Di-iii). Cad. 3 expression in this blastoporal domain appears to expand into a broader oral expression pattern in the late planula stage, and is maintained at higher levels relative to the rest of the embryo (Fig. 2Div).

2.2. Cadherin 1 is more highly expressed following the onset of gastrulation, in the forming endoderm and in an aboral domain

Cad. 1 expression was undetectable by *in situ* hybridization in early cleavage stages compared to Cad. 3 (Fig. 2Ei), but becomes much higher at the onset of gastrulation in a domain inside the invaginating blastopore (Fig. 2Eii). This domain appears to be restricted to the internal pre-endodermal plate and excluded from the blastopore lip ectoderm, and persists throughout gastrulation (Fig. 2Eiii). Beginning in the early planula stage, a second domain of Cad. 1 expression is detected at the aboral tip of the embryo and expands orally as development progresses (Fig. 2Eiv; white arrow). At the late planula stage, there appears to be a discrete boundary between the high level of expression of Cad. 3 in the oral ectoderm, and the expression pattern of Cad. 1 in the medial and aboral ectoderm (Fig. 2Div & Evi; black arrows); it should be noted that Cad. 3 expression is present in the aboral ectoderm, although at a lower level than in the oral ectoderm.

2.3. α-Catenin, β-catenin, and Cad. 3 co-localize to apical cell-cell junctions in the early embryo

We investigated the subcellular localization of α-catenin, β-catenin and Cad. 3 using mRNAs encoding fluorescent fusion proteins. mRNAs were co-injected into fertilized eggs, and fluorescent protein localizations were detected at the blastula stage by confocal fluorescence microscopy. Proteins encoded by mRNAs of α-catenin: mNeonGreen (Fig. 2Ei), β-catenin: mTagBFP2 (Fig. 2Eii), and Cad.3: mScarlet (Fig. 2Eiii) co-localized to cell-cell contacts at the boundary of the lateral and apical membrane of all cells in the blastula. Prominent staining of all proteins was also detected at tri-cellular junctions between cells.

2.4. Perturbation of the cadherin-catenin complex by knockdown of α-catenin produces variable gastrulation defects that emerge after the onset of gastrulation

α-Catenin was used as an experimental proxy to assay for a function of the CCC in cell adhesion due to its key role as a structural link between intercellular cadherin adhesions and the internal actin cytoskeleton at the Adherens Junction in bilaterian model systems (Herrenknecht et al., 1991; Rimm et al., 1995). RNA interference (RNAi) using short-hairpin RNAs has recently been demonstrated to be an effective strategy for experimental gene perturbation in *Nematostella* (He et al., 2018); due to its efficiency and ease of use, we chose to use a similar approach using short interfering RNAs (siRNAs). To validate this methodology, we first targeted a gene, FGFa2, previously knocked down using morpholinos – preliminary experiments showed that micro-injection of two separate test siRNAs to FGFa2 reproduced the previously published morpholino phenotypes (Rentzsch et al., 2008) (Supp. Fig. 2). Two siRNAs targeting different regions of the *Nv* α-catenin transcript were tested independently and in combination: microinjection of both siRNAs produced the most reproducible phenotype and the largest extent of knockdown, and this condition was therefore used in further experiments (Supp. Fig. 3).

The defects observed in α-catenin siRNA-injected embryos were variable, and appeared to be associated with gastrulation at 36 h.p.f., including: mild exogastrulation or blastoporal protrusion, and a general disorganization or lack of tissue integrity of the forming endoderm early in development (Fig. 3A). As corroborative, independent evidence, a series of α-catenin morpholino knockdown experiments were also carried out. The defects induced by morpholinos targeted to the start codon of α-catenin appeared to phenocopy those produced by α-catenin siRNAs (Fig. 3A). To quantify the timing and extent of siRNA-mediated gene knockdown, we performed a series of qPCR experiments over a developmental time-series; this revealed that α-catenin mRNA levels did not decrease substantially until later in development, and decreased gradually from 72.5% relative expression at 8 h.p.f. to 40.9% at 40 h.p.f. (Fig. 3B).

We explored two hypotheses to explain why a cohesive endodermal epithelium failed to form in α-catenin siRNA-injected embryos. We theorized that α-catenin knockdown caused either: (1) a breakdown in the mechanism of morphogenesis *before* gastrulation resulting in abnormal internalization of cells into the embryo; or (2) a structural compromise of the endodermal epithelium *after* gastrulation resulting from weakened cell-cell adhesions, or a loss of capacity to form new adhesions. To test whether gastrulation began normally by invagination, embryos were observed over a time course corresponding to the period from the onset of gastrulation (18 h.p.f.) to the time of contact between the pre-endodermal plate and the aboral end of the blastocoel (24 h.p.f.) (Fig. 3C). During this time, gastrulation appeared to begin normally by invagination in control and α-catenin siRNA-injected embryos. Minor defects in pharyngeal morphology were apparent in some α-catenin siRNA-injected embryos at 20 h.p.f., and a reduced blastocoelar space and partial delamination of the endodermal epithelium was evident at 24 h.p.f. (Fig. 3C). We quantified these data into 3 general phenotype categories at the completion of gastrulation: disordered endoderm, exogastrulation, and normal gastrula (Fig. 3D). The endodermal disorganization defect appeared to be the more robust defect in α-catenin siRNA-injected embryos (48.2%; n = 60 in 3 independent experiments). Exogastrulation (15.4% in α-catenin siRNA-injected embryos) may be a general injection phenotype as a similar percent of control injections (9.5%) had this defect (Fig. 3D).

By 2 d.p.f., clear defects in tissue organization in the endoderm were apparent in α-catenin siRNA-injected embryos. These defects were a general disorganization and delamination of the endoderm, which in severe cases appeared as a bolus of non-adherent cells (Fig. 3E). When viewed from the oral end of the embryo, the lack of endodermal tissue integrity appeared to result in a failure to form pre-mesentery pouches (blastoporal views; Fig. 3E). As development progressed into larval stages, α-catenin siRNA-injected embryos failed to produce normal musculature and mesenteries at 4 d.p.f., and subsequently failed to undergo normal metamorphosis and tentacle morphogenesis (Fig. 3F). At 10 d.p.f., when metamorphosis is complete in control fertilization cultures, a larger proportion of α-catenin siRNA-injected embryos either died or failed to undergo metamorphosis into normal polyps (23.1% abnormal and 53.7% dead: n = 100 in each of 3 independent experiments) compared to control embryos (9.8% abnormal and 13.7% dead; n = 100 in each of 3 independent experiments) (Fig. 3F).

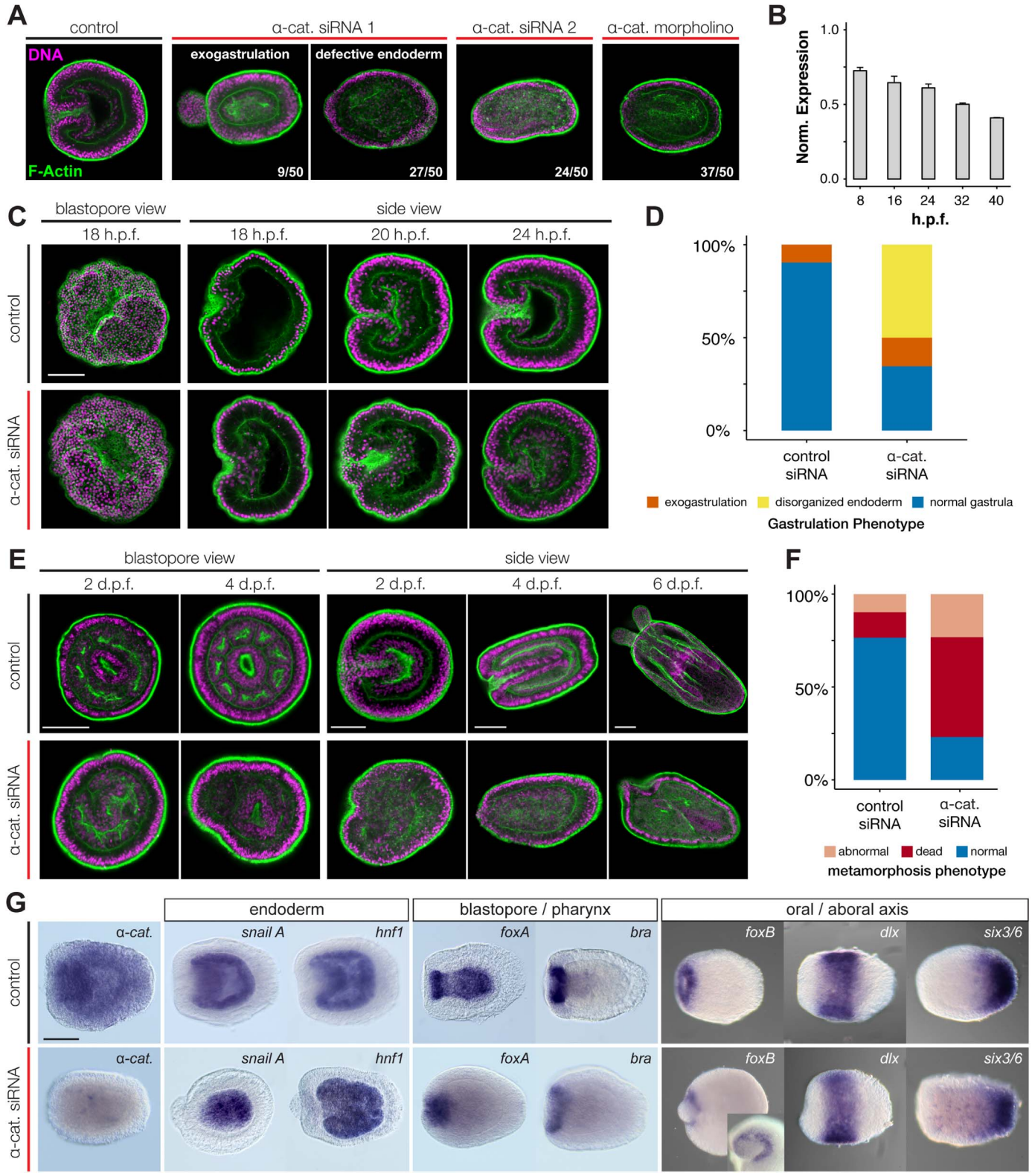

Fig. 3. knockdown of *Nv* α-Catenin produces gastrulation defects that disrupt metamorphosis. **A**. Embryos injected with α-catenin siRNAs or start codon-targeted morpholino versus control siRNA at 30 h.p.f., stained for DNA (propidium iodide, magenta), and F-Actin (Alexa-Fluor 488 Phalloidin, green). **B.** RT-qPCR analysis of *Nv* α-Catenin expression levels over time in embryos injected with a mixture of siRNA 1 and 2. **C, E.** Embryos injected with a 1:1 mixture of siRNAs versus control embryos across a series of developmental stages during gastrulation (**C**), and subsequent larval growth (**E**), stained as in **A. D**. quantification of phenotypes at 2 days post-fertilization. **F.** quantification of phenotypes at 10 days post-fertilization. **G.** *In situ* hybridization for endoderm (*snailA*, *hnf1*), gastrulation (*foxA*, *brachyury*), and axial patterning (*foxB*, *dlx*, *six3/6*) markers in treated versus control embryos at early planula stage. Scale bars are 50 μm throughout. (For interpretation of the references to color in this figure legend, the reader is referred to the web version of this article.)

We also tested whether defects in α-catenin siRNA-injected embryos were due to differences in the degree of knockdown of α-catenin expression within the embryo. We performed *in situs* for *Nv* α-catenin mRNA in control and α-catenin siRNA-injected embryos, and control and knockdown *in situs* were developed in parallel for the same amount of time in all experiments. The expression level of *Nv* α-catenin mRNA in α-catenin siRNA-injected embryos was generally much weaker than that in controls, with higher levels of expression evident only mosaically in a small number of cells (Fig. 3G).

Overall, these results indicate that the morphological defect in the endodermal epithelium in α-catenin siRNA-injected embryos was not due to a defect in cell movements that disrupted gastrulation, but occurred after normal gastrulation.

2.5. Gene expression analysis indicates normal patterning of the endoderm, blastopore, and primary body axis in α-catenin RNAi-injected embryos

The endodermal defect in α-catenin siRNA-injected embryos could be the result of the loss of the proper specification of the presumptive endoderm, or patterning of the blastopore or the primary body axis. This could be due to either indirect effects on conserved signaling functions of *Nv* β-catenin (Wikramanayake et al., 2003), or direct effects through a novel patterning role for α-catenin in *N. vectensis*. To test this hypothesis, we performed a series of *in situ* hybridizations of markers of tissue specification (Fig. 3G): the presumptive endoderm (*snailA* and *hnf1*; (Kirillova et al., 2018; Magie et al., 2007; Steinmetz et al., 2017)); patterning of the blastopore (*brachyury* and *foxA*; (Fritzenwanker et al., 2004; Martindale et al., 2004)); and, oral-aboral axial patterning (*foxB*, *dlx*, and *six3/6;* (Magie et al., 2005; Ryan et al., 2007; Sinigaglia et al., 2013)) (Fig. 3G).

In α-catenin siRNA-injected embryos, *SnailA* and *HNF1* appeared to be expressed normally in internalized cells, although in cases where blastoporal protrusions were evident neither endodermal marker was expressed. *Brachyury* and *FoxA* appeared to be expressed normally around the blastopore, but normal pharyngeal expression was partially ablated. *FoxB*, *Dlx*, and *Six3/6* are transcription factors with oral, medial, and aboral domains of ectodermal expression, respectively, and all three were expressed in their normal positions along the oral-aboral axis. However, blastoporal protrusions were within the ring of oral *FoxB* expression indicating that this tissue is not expanded, externalized pharyngeal ectoderm. In some cases, small patches of *Six3/6* expression was observed more orally in α-catenin siRNA-injected embryos compared to the normal restricted distribution in aboral domains (Fig. 3G).

These results indicate that α-catenin siRNA knockdown generally produced normally patterned embryos with an intact oral-aboral axis and properly specified, internalized endoderm. These embryos were capable of swimming for several days, but were ultimately non-viable and failed to undergo metamorphosis into primary polyps. Thus, the main phenotype produced by RNAi knockdown of α-catenin may be a mechanical failure that caused delamination of the endodermal epithelium after the onset of gastrulation, which resulted in an internal mass of non-adherent cells in place of a coherent tissue.

2.6. Cell adhesion is inhibited by α-catenin knockdown and removal of calcium in an ex vivo cell aggregation assay

We sought to determine whether the apparent restriction of the embryonic α-catenin knockdown phenotype to the endoderm was due to a tissue-specific difference in the role of α-catenin, or due to other factors, such as mechanical differences between ectoderm and endoderm. We hypothesized that if α-catenin has a general role in cell-cell adhesion across all embryonic tissues, which may have been masked in ectodermal cells, then the re-formation of cell-cell adhesions from dissociated whole embryos containing both ectodermal and endodermal cells should be inhibited. To test this, we used a well-characterized, quantitative cell adhesion assay in which dissociated cells are allowed to re-aggregate in a hanging drop (Benjamin et al., 2010; Ehrlich et al., 2002). This approach is supported by previous studies showing that embryonic cells isolated from *Nematostella* gastrulae have a remarkable capacity to aggregate, epithelialize, and re-pattern (Kirillova et al., 2018).

To investigate embryonic adhesion, a standard number of early gastrula stage embryos was collected in an equivalent volume of 1/3ASW, and subsequently triturated in calcium-magnesium-free artificial sea water (CMF) (see Materials and Methods). Dissociated cells were then pipetted into droplets of media of standardized volumes onto the underside of petri dish lid, and were allowed to aggregate over time by gravity. At one hour intervals cells were disrupted with mild trituration using a standard number of pumps through a p200 pipette tip to measure the robustness of forming cell-cell aggregates (Fig. 4A).

Cells isolated from α-catenin siRNA-injected embryos had a reduced capacity to re-aggregate over the course of 4 h compared to cells from control embryos in normal 1/3 FSW media; in general, < 10% α-catenin siRNA-injected cells formed small aggregates of < 6–25 cells, whereas 50% of control cells formed aggregates of > 11–50 cells, with larger aggregates (50+ cells) increasing in frequency over time (Fig. 4B). α-Catenin siRNA-injected cells formed more aggregates than a baseline positive control of control cells placed in media lacking calcium (1/3CMF supplemented with 1 mM EDTA) (Fig. 4B, C). The morphologies of cell aggregates from α-catenin siRNA-injected and control cells grown for 48 h were different: α-catenin siRNA-injected cell aggregates were generally smaller in size with a looser appearance with rounded cells, and less clearly defined tissue organization than control cell aggregates (Fig. 4D). There was also a difference in the mean number of successful aggregates formed per droplet between treatments, with the α-catenin siRNA-injected cells forming fewer aggregates than in negative control conditions (siRNA: 0.8 ± 0.1, control: 4.1 ± 0.1; n = 60 in each of 3 independent experiments; Fig. 4E).

Following the observation that calcium is necessary for cell re-aggregation, we tested whether calcium is generally necessary for cell-cell adhesion by placing intact embryos into CMF media. In calcium-free conditions in the presence of EDTA, the epithelial cells of early gastula embryos gradually dissociated from each other within 5–6 h without any trituration or enzymatic treatment (Fig. 4Fi-iii; full time series in Supp. Fig. 4). Analysis of the actin cytoskeleton by phalloidin staining and confocal microscopy in CMF-treated embryos revealed that cell dissociation began with the separation at the apical cortices of neighboring cells (arrow, Fig. 4G), and continued as cells became rounded and maintained connections by thin, filamentous projections (Supp. Fig. 5).

We exploited the requirement of extracellular calcium for adhesion in *N. vectensis* embryos to test whether weakening cell-cell adhesions could phenocopy the observed defects of α-catenin siRNA treatment. In order to approximate a weak or inhibited cell-cell adhesion phenotype during gastrulation, control embryos were treated with CMF media without supplemental EDTA at the onset of gastrulation (18 h.p.f.) for 24 h. In comparison to untreated control embryos that formed normal gastrula (Fig. 4Hi), CMF-incubated embryos had a variety of gastrulation defects, including exogastrulation, arrested gastrulation, and formation of a disorganized endoderm (Fig. 4Hii-iv). Although the morphology of these phenotypes was different from the α-catenin knockdown phenotypes, significantly a non-adherent or disorganized endoderm was the predominant phenotype observed (32% arrested gastrulation, 47% disorganized endoderm, and 18% exogastrulation in CMF-treated embryos, versus 1%, 4%, and 3% in control embryos, respectively, n = 50 in each of 3 independent experiments; Fig. 4I).

These results indicate that there is a generalized defect in cell-cell adhesion in α-catenin siRNA-injected embryos, and that this defect was phenocopied by defects in cell-cell adhesion in control embryos incubated in the absence of calcium. These properties are consistent

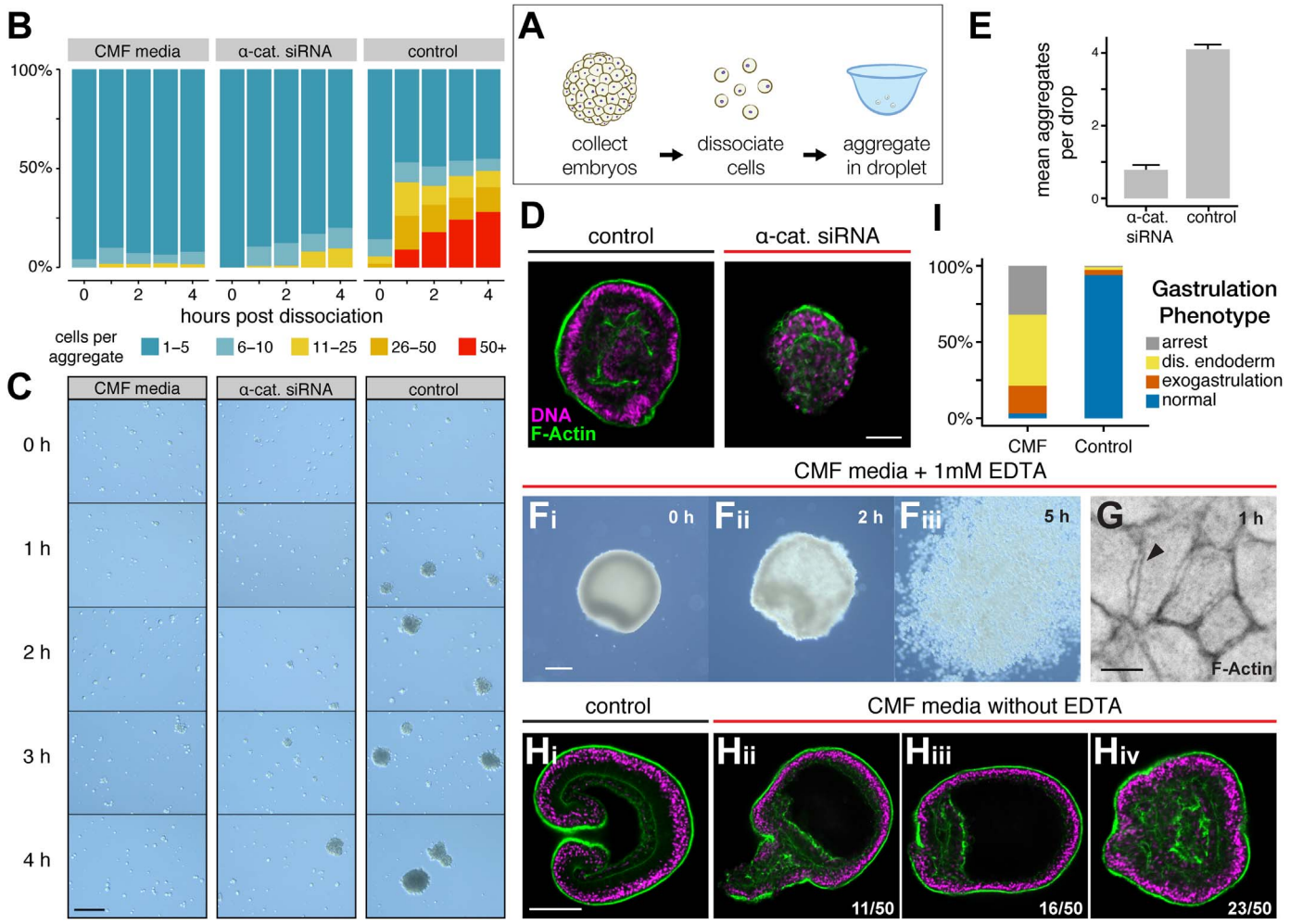

Fig. 4. *Nv* α-catenin is necessary for cell adhesion and the formation of epithelial tissues. **A.** Schematic of the hanging drop cell adhesion assay. **B.** quantification of hanging drop assay indicating the number of cells in different size classes of aggregates formed over time. Data is representative of 3 independent assays. **C.** representative images of cell aggregate formation observed in the hanging drop assay. **D.** representative images of epithelial cell aggregates formed after 48 h in a hanging drop. **E.** quantification of the mean number of aggregates formed per droplet after 48 h. **Fi-iii.** Representative images from a 6-h time series of an embryo treated with calcium-magnesium free media plus 1 mM EDTA at the onset of gastrulation. **G.** 40x confocal image of the apical cell surface of a phalloidin-stained embryo after 1 h of CMF + EDTA treatment. Arrow indications forming separation between F-actin cortices of adjacent cells. **Hi-v.** representative images of variable gastrulation phenotypes observed in embryos treated with CMF media without additional EDTA versus untreated control embryos. **I.** Quantification of the proportion of phenotypes observed in the CMF without EDTA treatments. Scale bars are 50 μm in C, D, F, and H, and 5 μm in G.

with the requirement for the mechanical functions of a calcium-dependent CCC in early *N. vectensis* development.

3. Discussion

3.1. Nv α-Catenin, β-catenin, and Cad. 3 form a potential CCC in the early embryo of N. vectensis

The observation that α- and β-catenin and Cad. 3 are co-expressed in all cells of the early embryo and co-localize to epithelial cell-cell junctions is indicative of a general and ubiquitous role for the CCC in cell-cell adhesion in *N. vectensis*. These observations are consistent with previous descriptions of membrane localization of α- and β-catenin in *N. vectensis* using a fusion mRNA strategy (Ragkousi et al., 2017; Wikramanayake et al., 2003), similar to that employed here, and a cross-reactive antibody against mammalian β-catenin (Leclère et al., 2016). In addition, α- and β-catenin proteins interact directly with both Cad. 3 and Cad. 1 to form a ternary complex *in vitro* (Clarke et al., 2016). Together, these results provide direct evidence of co-localization and high-affinity binding of proteins of the *N. vectensis* CCC, indicating the presence of a *bonefide* CCC at cell-cell contacts in *N. vectensis* epithelial tissues.

3.2. Dynamic expression patterns suggest different roles for classical cadherins in Nematostella early embryogenesis

A striking result from our *in situ* hybridizations is the difference in expression patterns between Cad. 3 and Cad. 1 in *N. vectensis* embryos. Cad. 3 mRNA was highly abundant in early cleavage stages. In contrast, Cad. 1 expression was very low or absent in early cleavage stages, although low levels of Cad. 1 transcripts have been reported in the fertilized zygote (Fischer et al., 2014; Tulin et al., 2013) which may have been below the sensitivity of our assay. Later in development, high levels of Cad. 3 expression became restricted to the blastopore lip and pharyngeal ectoderm in the early planula stage. In contrast, initial Cad. 1 expression was restricted to the internal pre-endodermal plate and excluded from the blastopore lip ectoderm during gastrulation, and then later at the aboral pole, expanding more orally as development progressed in early planula stages. The endodermal Cad. 1 expression pattern fits with a previous observation that Cad. 1 is in a co-regulated gene set identified in a screen for endodermal targets of antagonistic BMP2/4 and β-catenin/TCF/LEF signaling associated with the onset of gastrulation and the specification of endoderm (Wijesena et al., 2017). The regionalized ectodermal expression domains of *Nv* Cad. 3 and 1 at planula stages (Fig. 2Civ & Dvi) further suggest tissue differences

associated with larval growth or the elaboration of morphological structures at this stage: in normal development, the tentacle bulbs and body column develop from cells in the Cad.3- and Cad. 1 -positive domains, respectively (Fritz et al., 2013).

Thus, the expression patterns of Cad. 3 and Cad. 1 at gastrula and later stages appeared to be non-overlapping with discrete boundaries between them, suggesting that there may be either regional or tissue-level differences in cell-cell adhesive properties in *N. vectensis,* as has been observed in other systems in which cadherin sub-type switching occurs (Hatta et al., 1987; Maeda et al., 2005; Oda et al., 1998). The significance of the different cadherin expression patterns, however, is unclear – *Nv* Cad. 3 and Cad. 1 may be the products of a Cnidarian-specific gene duplication, and are not direct orthologs of cadherins from known cases of cadherin sub-type switching (Clarke et al., 2016). Therefore, further experiments will be needed to test whether of Cad. 3 and 1 are functionally distinct. Nevertheless, our expression data indicate that *Nv* Cad. 3 and Cad. 1 are interesting molecules worthy of future study, and that they may present a test case for studying differences in adhesive properties between cell types in a basally branching animal group.

3.3. Analysis of Nv α-catenin embryonic phenotypes and the potential for a CCC link to the cytoskeleton

RNAi and morpholino knockdown of α-catenin in *N. vectensis* produced endodermal tissue integrity phenotypes after the onset of gastrulation that are suggestive of a severe reduction or loss of cell-cell adhesion, rather than abnormalities in cell fate specification (Fig. 3). These phenotypes are similar to morphogenesis and adhesion defects in knockdown embryos after gastrulation in other invertebrates (Costa et al., 1998; Sarpal et al., 2012), but differ in timing compared to some vertebrate models in which knockdown resulted in developmental arrest prior to gastrulation (Kofron et al., 1997; Torres et al., 1997). This latter timing difference appears to be due to the timing of siRNA-mediated gene knockdown (Fig. 3B), but it may also be due to: (1) differing extents of maternal provisioning of α-catenin protein in the egg between species, as has been suggested previously (Sarpal et al., 2012); and (2) the large number of α-catenin paralogs with overlapping functions in vertebrates (Abe et al., 2004; Janssens et al., 2003; Park et al., 2002; Torres et al., 1997; Uchida et al., 1994), compared to the single α-catenin gene in *N. vectensis*. The delay in reduction of α-catenin mRNA levels we observed by qPCR is similar to results reported in the initial demonstration of RNAi in *N. vectensis* by He et al., which suggests that RNAi gene knockdown may generally be less active at earlier time-points in this species (He et al., 2018); this should be taken into consideration in future RNAi studies.

A challenge to the interpretation that *Nv* α-catenin has a general and ubiquitous role in embryonic cell-cell adhesion is the observation that the phenotype is predominantly manifested in the endoderm, and absent from the ectoderm. The difference in defects in the ectoderm and endoderm in α-catenin RNAi embryos could be due to differences in the efficacy of RNAi between ectoderm and endoderm in *Nematostella*. We note, however, that the control FGFa2 knockdown produced a strong ectodermal phenotype, indicating that RNAi is active in the ectoderm. Although the embryonic phenotype was most evident in the endoderm in the embryo, we detected a general cell adhesion role for α-catenin in our cell re-aggregation assays following whole embryo dissociation (Fig. 4), indicating that α-catenin knockdown likely affected ectodermal cell adhesion which may have been masked in the intact embryo.

It is possible that another protein plays a redundant function to α-catenin in the ectoderm. The *N. vectensis* genome encodes only one α-catenin ortholog, but encodes another member of the same gene family, vinculin. Although vinculin is more commonly associated with integrin-mediated cell-ECM adhesions (Bakolitsa et al., 2004; Plotnikov et al., 2012), it also localizes to the AJ in bilaterians and in sponges (Miller et al., 2018), and has been shown to perform a similar actin-binding function to α-catenin in vertebrates (le Duc et al., 2010; Peng et al., 2010). Further work will be necessary to understand whether vinculin plays a role in *N. vectensis* cell-cell adhesion.

Another plausible explanation for the predominant *in vivo* effect of α-catenin knockdown on the endoderm is that there are differences in the amount of mechanical stress in the ectoderm and endoderm in the *N. vectensis* embryo. Physical and mechanical differences in adhesive properties between embryonic tissues have been well-known documented (Holtfreter, 1947; Townes and Holtfreter, 1955), and a difference in mechanical stress has been reported between cells in general ectoderm (low mechanical stress) versus cells in the blastopore lip ectoderm (high mechanical stress) at the onset of gastrulation in *Nematostella* (Pukhlyakova et al., 2018). Thus, in the embryo, lower mechanical stress in the ectoderm could mask a cell-cell adhesion defect produced by α-catenin knockdown. Further analysis of the mechanical properties of these tissues at later developmental time-points will be necessary to test this hypothesis.

Finally, these findings are somewhat inconsistent with recent work from Salinas-Saavedra et al., who observed morphological differences in cell junctions between ectoderm and endoderm using transmission electron microscopy, and detected an apparent lack of β-catenin protein localization in endoderm using immunohistochemistry (Salinas-Saavedra et al., 2018). Their results challenged the idea that the cadherin-catenin complex is needed for the formation of adherens junctions in *N. vectensis* endoderm. However, our observations are consistent with the original report of *N. vectensis* β-catenin by Wikramanayake et al., who observed ubiquitous localization of β-catenin protein, including strong staining within the endoderm, using a different anti-β-catenin antibody (Wikramanayake et al., 2003). Rigorous molecular characterization of junctional protein complexes in both endoderm and ectoderm will be necessary to resolve this discrepancy; such work will likely be highly informative to our understanding of the evolution of epithelial tissues.

3.4. Calcium dependence of cell adhesion in N. vectensis is consistent with a role for cadherins

Our experiments on embryos and cells placed into calcium-free conditions demonstrate that calcium, and likely classical cadherins, are necessary for both the maintenance of embryonic cell-cell adhesions, as well as the formation of new adhesions in re-aggregating cells (Fig. 4; Supp. Fig. 4 and 5). This result is consistent with observations of early embryos from other invertebrates in which removing calcium is sufficient to dissociate embryos (Herbst, 1900; McClay, 1986), and the initial work in mammalian cell culture that led to the discovery of cadherins as calcium-dependent cell adhesion molecules (Takeichi, 1977). However, we cannot exclude the possibility that other adhesion systems are also involved, including extracellular matrix (ECM) proteins (Fidler et al., 2017) that contribute to cell adhesion and aggregation in sea urchin embryos (McClay, 1986), sponge tissues (Haseley et al., 2001; Henkart et al., 1973; Müller and Zahn, 1973), and unicellular animal relatives such as the amoeba-like filasterean *Capsaspora owczarzaki* (Sebé-Pedrós et al., 2013) and the choanoflagellate *Salpingoeca rosetta* (Levin et al., 2014). Further experiments on *N. vectensis* and other non-bilaterian model systems will be necessary to assess the relative importance of cadherin-based cell-cell adhesion versus cell-ECM adhesion for tissue integrity and organization in early animals.

The embryological data presented here suggest that *Nv* α-catenin has a conserved function linking cadherin adhesions to the cytoskeleton, and, therefore, that the CCC is involved in coordinating calcium-dependent cell adhesion in cnidarians. Taken together with other observations of conserved functions for CCC components in *N. vectensis* (Clarke et al., 2016; Pukhlyakova et al., 2018; Wikramanayake et al., 2003), our work further demonstrates the deep

ancestry of the CCC as a cell-cell adhesion complex and signaling module. Further study is necessary in cnidarians to more fully understand the basis of cell-cell adhesion in this phylum and how it may differ between tissues and across developmental time. Additionally, more data on cell-cell adhesion from other basally branching phyla, including ctenophores, sponges, and placozoans will be necessary to understand how changes in adhesive mechanisms during early animal evolution impacted the evolution of animal multicellularity.

4. Materials and methods

4.1. Animal culture, procurement and microinjection of embryos

N. vectensis polyps and embryos were cultured at Hopkins Marine Station, Stanford University, under conditions similar to previous studies (Fritzenwanker and Technau, 2002; Hand and Uhlinger, 1992). Briefly, adult male and female anemones were kept in isolated cultures under constant darkness at 18 °C in 1/3x filtered sea water media (1/3 FSW), and received a daily water change and feeding of brine shrimp. Spawning was induced with a 6-h heat and light treatment in a climate-controlled incubator, and collected egg masses were de-jellied by gentle oscillation in a solution of 4% L-cysteine in 1/3 FSW (w/v) for 15 min. Eggs were washed five times with 1/3 FSW and fertilized within 2 h of spawning. Microinjection was carried out as described previously (Layden et al., 2013); briefly, de-jellied eggs were plated in rows in a plastic petri dish and then injected using a 3-axis joystick micromanipulator (MO-202U, Narishige) and a microinjection system (MPPI-3, Applied Scientific Instrumentation) on a Zeiss V12 Discovery stereoscope under epifluorescence. Following injection and fertilization, embryo cultures were maintained at 18 °C in 1% agarose-coated petri dishes.

4.2. Nomenclature and gene annotations of Nematostella cadherins

To avoid confusion in the literature, we have used the gene names from the original annotation of cadherin gene models from the *Nematostella* genome, NvCdh3 and NvCdh1, as described by Hulpiau and van Roy (Hulpiau and van Roy, 2011). These genes correspond to the annotations *Nv*Cadherin-1 and *Nv*Caderhin-2, respectively, as described in our previous work (Clarke et al., 2016).

4.3. Molecular cloning and reagent preparation

For mRNA injection experiments, full-length coding sequences of α-catenin and β-catenin were amplified from cDNAs and cloned into a modified pCS2 vector to form in-frame fusions with mNeonGreen, or mTagBFP2 coding sequences using Gibson assembly (Gibson et al., 2009). For Cad. 3, a 12-kb partial coding sequence corresponding to the 14 membrane-proximal CAD repeats, transmembrane domain, and cytoplasmic tail was cloned and fused to mScarlet using a similar strategy. Clones for α-cat., β-cat., Cad. 1, Cad. 3, HNF1, SnailA, Brachyury, and FoxA were prepared by standard PCR and TA cloning protocols using the pGEMT-Easy vector system (Promega). cDNAs for FoxB, Dlx, and Six3/6 were a gift from Mark Martindale. mRNA was transcribed *in vitro* from linearized plasmid templates using the T7 ARCA transcription kit (New England Biolabs). Digoxigenin-labeled anti-sense RNA probes for *in situ* hybridization were transcribed using SP6 or T7 RNA polymerase (Promega). Sequences for all primers used for cloning in this study are included in Table 1.

4.4. siRNAs and morpholino antisense oligonucleotides

siRNAs were ordered from IDT and 100 μM stock dilutions were prepared according to the Manufacturer's instructions in nuclease-free water. Two siRNAs against α-catenin were used in this study comprising a CDS-targeted siRNA targeting base positions 671–696 and another targeting the 3′UTR (full sequences in Table 2). For microinjection, siRNAs were diluted to 20 μM and co-injected (40 μM total concentration) in an injection mix supplemented with 0.5 mg/ml rhodamine-dextran and 100 mM Na^+ in nuclease-free water. Control embryos were injected with either a non-sense siRNA with a scrambled sequence of similar composition to the 3-UTR-targetted siRNA for α-catenin knockdown experiments ('control'; Table 2), or a rhodamine dextran blank for the FGFa2 validation experiments. A morpholino targeted to the start codon of α-catenin (sequence: 5′-TG GTAGGCCGTCCGACTCATTTTCG-3′) was ordered from Gene Tools, LLC, resuspended following the manufacturer's instructions, and diluted to 500 μM in the final injection mix.

Table 1
Primer sequences used for cloning in this study. Primers used to isolate clones for in situ hybridization are designated 'ISH', and those for preparing mRNA transcription vectors are designated 'mRNA'. Where present, lowercase sequence indicates the portion of the primer with homology to the vector backbone used for Gibson Assembly.

NvAcat_ISH_F	CTCCGCAAGCCCCGTCTAT
NvAcat_ISH_R	GAACTCGCTTAGTGCTTGAATAGGA
NvBcat_ISH_F	CTGCAGAGCTTGTGCGTATCA
NvBcat_ISH_R	GGAAGAGCGAGCTGGTCAAC
NvFoxA_ISH_F	CCTACTACATTACCCTTCCAGCAC
NvFoxA_ISH_R	CCGTTCCCTCGCCTGAC
HNF1_ISH_F	CAACCGAGCTACAGAGAGAGC
HNF1_ISH_R	GCCACGCACATATAGTAGCCAC
NvSnailA_ISH_F	GACACACAGACCTCGGACAAG
NvSnailA_ISH_R	TCCCTTGGATAATGTGAATAGCCTC
NvBra_ISH_F	ACATGCACTCGGACGAGAAG
NvBra_ISH_R	TTAAGCTTGCGGTATGGTGTTCC
Nv_Acat_mRNA_F	agaagctcagaataaacgctcaactttggcATGAGTCGGACGGCCTACC
Nv_Acat_mRNA_R	catcgatgctcctgaggctcccgatgctccGTAGAAGTCGGGCTTCCGTC
Nv_Bcat_mRNA_F	agaagctcagaataaacgctcaactttggcATGGAGACACACGGTATGG
Nv_Bcat_mRNA_R	catcgatgctcctgaggctcccgatgctccGAGATCTGTGTCATACAGAGG
Nv_Cad3_mRNA_F	agaagctcagaataaacgctcaactttggcATGATTTCTACGCTTGGTCG
Nv_Cad3_mRNA_R	catcgatgctcctgaggctcccgatgctccGTCGTCAAGGTTGTAGATCT

4.5. RT-qPCR analysis of gene expression

RT-qPCR was used to assess α-catenin mRNA levels. For each experiment, 30 treated embryos and 30 control embryos were collected into two tubes, and RNA was isolated from the pooled embryos using a RNAqueous Micro RNA isolation kit (Life Technologies). RNA samples were analyzed directly using Luna Universal One-Step RT-qPCR master mix (New England Biolabs) in a Mic qPCR cycler (Bio Molecular Systems); 20 μl reactions were set up in triplicate for each sample and run according to the manufacturers specifications. The Nematostella genes *ATP synthase*, *EF1b*, and *RPL23* were used as control standards for all experiments. A minimum of three biological replicates were used for each treatment or time-point. Sequences of all primers used for qPCR analysis are reported in Table 3.

4.6. Whole mount in situ hybridization, nuclear and F-actin staining

In situ hybridization was performed as described previously (Lowe et al., 2004; Wolenski et al., 2013). RNA probes were diluted to 0.1 – 0.5 ng/ml and hybridized overnight at 60 °C, and visualized using an Anti-DIG AP antibody and NBT/BCIP (Roche). F-actin and nuclei were stained as described previously (Magie et al., 2007); embryos were co-incubated with a 1:50 dilution of Alexa-Fluor 488 conjugated phalloidin and a 1:200 dilution of propidium iodide plus 1:500 20 mg/ml RNAse A at room temperature in PT buffer for 1 h, dehydrated quickly through an isopropanol series (30%, 60%, 90%, 3 ×100%), and transitioned into Murray's Clear media (2:1 benzyl benzoate and benzyl alcohol).

Table 2
siRNA sequences used in this study.

Gene Target	Target Location	Base position	sense sequence
α-Cat.	CDS	671–696	rGrCrArArArArUrGrCrUrUrCrUrArUrCrUrUrCrUrUrCrCAA
α-Cat.	3′UTR	3939–3964	rArUrCrUrUrGrArArUrGrArArUrArCrUrArGrArArArUrGTT
control	NA	NA	rGrUrCrArArGrArUrArUrUrGrArUrGrArCrArGrArArUrUGT
FGFa2	CDS	303–328	rCrArGrArUrArUrGrCrCrCrUrArArUrGrArArArArUrCrGAG
FGFa2	CDS	187–212	rGrArArArArArArUrUrCrUrArCrCrGrCrCrArArCrArUrCTT

Table 3
Primer sequences used for qPCR in this study.

Nv_ATPsynt_qPCR_F	TGCTGGGAAAGTTCTGGACCAATG
Nv_ATPsynt_qPCR_R	ACACCCTCCTTGACGGTAACATTC
Nv_EF1b_qPCR_F	TGCTGCATCAGAACAGAAACCTGC
Nv_EF1b_qPCR_R	TAAGCCTTCAAGCGTTCTTGCCTG
Nv_RPL23_qPCR_F	TTACGGAGCTCTGGCTTTCCTTTC
Nv_RPL23_qPCR_R	TGCCGTTAAGGGTATCAAAGGACG
Nv_Acat_qPCR_F	CTAGTGGAGACGTGAAAGTTGAG
Nv_Acat_qPCR_R	GGTTTACCAGAGTTGTCACCTG

4.7. Cell dissociation and aggregation

Cell dissociation was performed as described previously (Kirillova et al., 2018). 100 embryos were collected in a microcentrifuge tube in 100 µl 1/3 FSW, two volumes of calcium-magnesium-free arfticial sea water (CMF-ASW: 27 g/L NaCl, 1 g/L Na2SO4, 0.8 g/L KCI, 0.18 g/L NaHCO3 in MilliQ water) was added, and embryos were dissociated via trituration through a p200 pipette tip. Following dissociation, cells were passed through a 40 µm cell strainer, collected via centrifugation for 3 min at 700 × g, washed three times into treatment medias, and re-suspended in 500 µl of media. Volumes used and number of embryos were kept constant across all treatments and experiments to control for input cell number. 1/3 calcium-magnesium-free (1/3 CMF) media was prepared by dilution of CMF-ASW with MilliQ water and the addition of 1 mM EDTA. EDTA was included in all CMF-media treatments unless otherwise indicated (as in Fig. 3I). The hanging drop assay was adapted from previous tissue culture studies

(Benjamin et al., 2010{Ehrlich, 2002 #518; Ehrlich et al., 2002). In brief, dissociated cells were pipetted in 20 µl droplets onto the underside of a petri dish lid and inverted to allow cells to aggregate due to gravity. At the indicated time points, droplets were triturated with 5 pumps through a p200 tip, spread on a slide, and 4 µl of 16% paraformaldehyde was added. 10 images were taken from random non-overlapping areas of the coverslip using a per droplet analyzed. Images were analyzed programmatically using ImageJ software (NIH). Each aggregation experiment was done in triplicate, and repeated for a minimum of three independent trials.

Embryonic CMF treatments were carried out by washing embryos 3 times in 1/3 CMF before placing them into petri dish containing treatment media. Phalloidin staining on CMF-treated embryos was done after gently pipetting embryos with a p1000 tip cut with a wide bore into a pre-fixation of 16% paraformaldehyde in 1/3 FSW and pre-fixing embryos for 5 min. before transitioning into normal fixation in 4% paraformaldehyde. Whole-embryo CMF treatments were repeated in three independent trials of 50 or more embryos each.

4.8. Imaging

All fluorescent images were captured with a Zeiss LSM 700 confocal microscope and either 20x air or 40x water-immersion objectives using the Zen software package (Carl Zeiss). mRNA-injected embryos were immobilized in 1% low-melting point agarose (Sigma) in a poly-L-lysine-treated coverslip-bottom imaging dish as described previously (Ragkousi et al., 2017). *In situ* hybridizations were imaged on either a Zeiss V12 Discovery dissection microscope using a 5x objective, or a Zeiss Z1 compound microscope with a 20x objective. The hanging drop assay and embryo dissociation experiment were imaged on the same compound scope using a 10x objective.

Acknowledgements

We thank Matthew Gibson and members of his laboratory for advice and training, Miguel Salinas-Saavedra and Mark Martindale for sharing protocols and *in situ* clones, and members of the Lowe and Nelson laboratories for helpful discussions. The personal communication in our introduction refers to a manuscript preprint (doi: http://dx.doi.org/10.1101/488270). Laboratory stock of *N. vectensis* was established with a gift of anemones from Kevin Uhlinger. We thank Kevin Uhlinger and Kathi Ishizuka for training and helpful discussions on animal husbandry. We thank Cody Dawson and Auston Rutledge for their work maintaining animal cultures, and Miranda Vogt for laboratory assistance with cloning mRNA constructs. This work was supported by a NSF (National Science Foundation, United States) Graduate Research Fellowship (DGE-114747 to DNC), and grants from the NIH (National Institutes of Health, United States) (R35GM118064, WJN), NSF (1258169, CL), NASA (National Aeronautics and Space Administration, United States) (15-EXO15_2–0027, CL), and the Dr. Earl H. Myers and Ethel M. Myers Oceanographic and Marine Biology Trust (DNC). The authors declare that there are no conflicts of interest with the contents of this article.

Appendix A. Supplementary material

Supplementary data associated with this article can be found in the online version at doi:10.1016/j.ydbio.2019.01.007.

References

Abe, K., Chisaka, O., Van Roy, F., Takeichi, M., 2004. Stability of dendritic spines and synaptic contacts is controlled by alpha N-catenin. Nat. Neurosci. 7, 357–363.
Abedin, M., King, N., 2008. The premetazoan ancestry of cadherins. Science 319, 946–948.
Abedin, M., King, N., 2010. Diverse evolutionary paths to cell adhesion. Trends Cell Biol. 20, 734–742.
Aberle, H., Schwartz, H., Kemler, R., 1996. Cadherin-catenin complex: protein interactions and their implications for cadherin function. J. Cell. Biochem. 61, 514–523.
Bakolitsa, C., Cohen, D.M., Bankston, L.A., Bobkov, A.A., Cadwell, G.W., Jennings, L., Critchley, D.R., Craig, S.W., Liddington, R.C., 2004. Structural basis for vinculin activation at sites of cell adhesion. Nature 430, 583–586.
Belahbib, H., Renard, E., Santini, S., Jourda, C., Claverie, J.-M., Borchiellini, C., Le Bivic, A., 2018. New genomic data and analyses challenge the traditional vision of animal epithelium evolution. BMC Genom. 19, 393.
Benjamin, J.M., Kwiatkowski, A.V., Yang, C., Korobova, F., Pokutta, S., Svitkina, T., Weis, W.I., Nelson, W.J., 2010. AlphaE-catenin regulates actin dynamics independently of cadherin-mediated cell-cell adhesion. J. Cell Biol. 189, 339–352.
Borghi, N., Sorokina, M., Shcherbakova, O.G., Weis, W.I., Pruitt, B.L., Nelson, W.J., Dunn, A.R., 2012. E-cadherin is under constitutive actomyosin-generated tension that is increased at cell-cell contacts upon externally applied stretch. Proc. Natl. Acad. Sci. USA 109, 12568–12573.
Buckley, C.D., Tan, J., Anderson, K.L., Hanein, D., Volkmann, N., Weis, W.I., Nelson, W.J., Dunn, A.R., 2014. The minimal cadherin-catenin complex binds to actin filaments under force. Science, 346.
Cereijido, M., Contreras, R., Shoshani, L., 2004. Cell adhesion, polarity, and epithelia in the dawn of metazoans. Physiol. Rev. 84, 1229–1262.
Clarke, D.N., Miller, P.W., Lowe, C.J., Weis, W.I., Nelson, W.J., 2016. Characterization of

the cadherin–catenin complex of the sea anemone nematostella vectensis and implications for the evolution of metazoan cell–cell adhesion. Mol. Biol. Evol. 33, 2016–2029.
Costa, M., Raich, W., Agbunag, C., Leung, B., Hardin, J., Priess, J.R., 1998. A putative catenin-cadherin system mediates morphogenesis of the Caenorhabditis elegans embryo. J. Cell Biol. 141, 297–308.
Dayel, M.J., Alegado, R.A., Fairclough, S.R., Levin, T.C., Nichols, S.A., McDonald, K., King, N., 2011. Cell differentiation and morphogenesis in the colony-forming choanoflagellate Salpingoeca rosetta. Dev. Biol. 357, 73–82.
Dickinson, D.J., Nelson, W.J., Weis, W.I., 2011. A polarized epithelium organized by beta- and alpha-catenin predates cadherin and metazoan origins. Science 331, 1336–1339.
Ehrlich, J.S., Hansen, M.D., Nelson, W.J., 2002. Spatio-temporal regulation of Rac1 localization and lamellipodia dynamics during epithelial cell-cell adhesion. Dev. Cell 3, 259–270.
Fairclough, S.R., Dayel, M.J., King, N., 2010. Multicellular development in a choanoflagellate. Curr. Biol. 20, R875–R876.
Fidler, A.L., Darris, C.E., Chetyrkin, S.V., Pedchenko, V.K., Boudko, S.P., Brown, K.L., Gray Jerome, W., Hudson, J.K., Rokas, A., Hudson, B.G., 2017. Collagen IV and basement membrane at the evolutionary dawn of metazoan tissues. eLife 6, e24176.
Fischer, A.H.L., Mozzherin, D., Eren, A.M., Lans, K.D., Wilson, N., Cosentino, C., Smith, J., 2014. SeaBase: a multispecies transcriptomic resource and platform for gene network inference. Integr. Comp. Biol. 54, 250–263.
Fritz, A.E., Ikmi, A., Seidel, C., Paulson, A., Gibson, M.C., 2013. Mechanisms of tentacle morphogenesis in the sea anemone Nematostella vectensis. Development 140, 2212–2223.
Fritzenwanker, J.H., Genikhovich, G., Kraus, Y., Technau, U., 2007. Early development and axis specification in the sea anemone Nematostella vectensis. Dev. Biol. 310, 264–279.
Fritzenwanker, J.H., Saina, M., Technau, U., 2004. Analysis of forkhead and snail expression reveals epithelial–mesenchymal transitions during embryonic and larval development of Nematostella vectensis. Dev. Biol. 275, 389–402.
Fritzenwanker, J.H., Technau, U., 2002. Induction of gametogenesis in the basal cnidarian Nematostella vectensis(Anthozoa). Dev. Genes Evol. 212, 99–103.
Gibson, D.G., Young, L., Chuang, R.-Y., Venter, J.C., Hutchison, C.A., III, Smith, H.O., 2009. Enzymatic assembly of DNA molecules up to several hundred kilobases. Nat. Methods 6, 343.
Grosberg, R.K., Strathmann, R.R., 2007. The evolution of multicellularity: a minor major transition? Annu. Rev. Ecol. Evol. Syst., 621–654.
Gumbiner, B.M., 2005. Regulation of cadherin-mediated adhesion in morphogenesis. Nat. Rev. Mol. Cell Biol. 6, 622–634.
Halbleib, J.M., Nelson, W.J., 2006. Cadherins in development: cell adhesion, sorting, and tissue morphogenesis. Genes Dev. 20, 3199–3214.
Hand, C., Uhlinger, K.R., 1992. The culture, sexual and asexual reproduction, and growth of the sea anemone nematostella vectensis. Biol. Bull. 182, 169–176.
Harris, T.J., Tepass, U., 2010. Adherens junctions: from molecules to morphogenesis. Nat. Rev. Mol. Cell Biol. 11, 502–514.
Haseley, S.R., Vermeer, H.J., Kamerling, J.P., Vliegenthart, J.F., 2001. Carbohydrate self-recognition mediates marine sponge cellular adhesion. Proc. Natl. Acad. Sci. 98, 9419–9424.
Hatta, K., Takagi, S., Fujisawa, H., Takeichi, M., 1987. Spatial and temporal expression pattern of N-cadherin cell adhesion molecules correlated with morphogenetic processes of chicken embryos. Dev. Biol. 120, 215–227.
He, S., del Viso, F., Chen, C.-Y., Ikmi, A., Kroesen, A.E., Gibson, M.C., 2018. An axial Hox code controls tissue segmentation and body patterning in Nematostella vectensis. Science 361, 1377–1380. http://dx.doi.org/10.1126/science.aar8384.
Helm, R.R., Siebert, S., Tulin, S., Smith, J., Dunn, C.W., 2013. Characterization of differential transcript abundance through time during Nematostella vectensis development. BMC Genom. 14, 266.
Henkart, P., Humphreys, S., Humphreys, T., 1973. Characterization of sponge aggregation factor. Unique proteoglycan complex. Biochemistry 12, 3045–3050.
Herbst, C., 1900. Über das Auseinandergehen von Furchungs-und Gewebezellen in kalkfreiem Medium. Arch. für Entwickl. der Org. 9, 424–463.
Herrenknecht, K., Ozawa, M., Eckerskorn, C., Lottspeich, F., Lenter, M., Kemler, R., 1991. The uvomorulin-anchorage protein alpha catenin is a vinculin homologue. Proc. Natl. Acad. Sci. USA 88, 9156–9160.
Holtfreter, J., 1947. Observations on the migration, aggregation and phagocytosis of embryonic cells. J. Morphol. 80, 25–55.
Hulpiau, P., van Roy, F., 2011. New Insights into the evolution of metazoan cadherins. Mol. Biol. Evol. 28, 647–657.
Janssens, B., Mohapatra, B., Vatta, M., Goossens, S., Vanpoucke, G., Kools, P., Montoye, T., van Hengel, J., Bowles, N.E., van Roy, F., Towbin, J.A., 2003. Assessment of the CTNNA3 gene encoding human alpha T-catenin regarding its involvement in dilated cardiomyopathy. Hum. Genet 112, 227–236.
Kane, D.A., Maischein, H.M., Brand, M., van Eeden, F.J., Furutani-Seiki, M., Granato, M., Haffter, P., Hammerschmidt, M., Heisenberg, C.P., Jiang, Y.J., Kelsh, R.N., Mullins, M.C., Odenthal, J., Warga, R.M., Nusslein-Volhard, C., 1996. The zebrafish early arrest mutants. Development 123, 57–66.
Kirillova, A., Genikhovich, G., Pukhlyakova, E., Demilly, A., Kraus, Y., Technau, U., 2018. Germ-layer commitment and axis formation in sea anemone embryonic cell aggregates. Proc. Natl. Acad. Sci..
Knoll, A.H., 2011. The multiple origins of complex multicellularity. Annu. Rev. Earth Planet. Sci. 39, 217–239.
Kofron, M., Spagnuolo, A., Klymkowsky, M., Wylie, C., Heasman, J., 1997. The roles of maternal alpha-catenin and plakoglobin in the early Xenopus embryo. Development 124, 1553–1560.
Larue, L., Antos, C., Butz, S., Huber, O., Delmas, V., Dominis, M., Kemler, R., 1996. A role for cadherins in tissue formation. Development 122, 3185–3194.
Larue, L., Ohsugi, M., Hirchenhain, J., Kemler, R., 1994. E-cadherin null mutant embryos fail to form a trophectoderm epithelium. Proc. Natl. Acad. Sci. USA 91, 8263–8267.
Layden, M.J., Rottinger, E., Wolenski, F.S., Gilmore, T.D., Martindale, M.Q., 2013. Microinjection of mRNA or morpholinos for reverse genetic analysis in the starlet sea anemone, Nematostella vectensis. Nat. Protoc. 8, 924–934.
le Duc, Q., Shi, Q., Blonk, I., Sonnenberg, A., Wang, N., Leckband, D., de Rooij, J., 2010. Vinculin potentiates E-cadherin mechanosensing and is recruited to actin-anchored sites within adherens junctions in a myosin II-dependent manner. J. Cell Biol. 189, 1107–1115.
Leclère, L., Bause, M., Sinigaglia, C., Steger, J., Rentzsch, F., 2016. Development of the aboral domain in *Nematostella* requires *β-catenin* and the opposing activities of *Six3/6* and *Frizzled5/8*. Development 143, 1766–1777.
Levin, T.C., Greaney, A.J., Wetzel, L., King, N., 2014. The rosetteless gene controls development in the choanoflagellate S. rosetta. Elife 3, e04070.
Lowe, C.J., Tagawa, K., Humphreys, T., Kirschner, M., Gerhart, J., 2004. Hemichordate embryos: procurement, culture, and basic methods. Methods Cell Biol., 171–194.
Maas, O., 1906. Über die Einwirkung karbonatfreier und kalkfreier Salzlösungen auf erwachsene Kalkschwämme und auf Entwicklungsstadien derselben. Arch. für Entwickl. der Org. 22, 581–599.
Maeda, M., Johnson, K.R., Wheelock, M.J., 2005. Cadherin switching: essential for behavioral but not morphological changes during an epithelium-to-mesenchyme transition. J. Cell Sci. 118, 873–887.
Magie, C.R., Daly, M., Martindale, M.Q., 2007. Gastrulation in the cnidarian Nematostella vectensis occurs via invagination not ingression. Dev. Biol. 305, 483–497.
Magie, C.R., Pang, K., Martindale, M.Q., 2005. Genomic inventory and expression of Sox and Fox genes in the cnidarian Nematostella vectensis. Dev. Genes Evol. 215, 618–630.
Martindale, M.Q., Pang, K., Finnerty, J.R., 2004. Investigating the origins of triploblasty: mesodermal'gene expression in a diploblastic animal, the sea anemone Nematostella vectensis (phylum, Cnidaria; class, Anthozoa). Development 131, 2463–2474.
McClay, D.R., 1986. Chapter 17. Embryo dissociation, cell isolation, and cell reassociation. In: Schroeder, T.E. (Ed.), Methods in Cell Biology. Academic Press, 309–323.
Miller, P.W., Clarke, D.N., Weis, W.I., Lowe, C.J., Nelson, W.J., 2012. The evolutionary origin of epithelial cell-cell adhesion mechanisms. Curr. Top. Membr. 72, 267–311.
Miller, P.W., Pokutta, S., Mitchell, J.M., Chodaparambil, J.V., Clarke, D.N., Nelson, W., Weis, W.I., Nichols, S.A., 2018. Analysis of a vinculin homolog in a sponge (phylum Porifera) reveals that vertebrate-like cell adhesions emerged early in animal evolution. J. Biol. Chem. 17, 001325, (jbc. RA117).
Misevic, G.N., Burger, M., 1993. Carbohydrate-carbohydrate interactions of a novel acidic glycan can mediate sponge cell adhesion. J. Biol. Chem. 268, 4922–4929.
Müller, W.E.G., Zahn, R.K., 1973. Purification and characterization of a species-specific aggregation factor in sponges. Exp. Cell Res. 80, 95–104.
Nagar, B., Overduin, M., Ikura, M., Rini, J.M., 1996. Structural basis of calcium-induced E-cadherin rigidification and dimerization. Nature 380, 360.
Nelson, W.J., 2008. Regulation of cell–cell adhesion by the cadherin–catenin complex. Biochem. Soc. Trans. 36, 149.
Nichols, S.A., Dirks, W., Pearse, J.S., King, N., 2006. Early evolution of animal cell signaling and adhesion genes. Proc. Natl. Acad. Sci. USA 103, 12451–12456.
Nichols, S.A., Roberts, B.W., Richter, D.J., Fairclough, S.R., King, N., 2012. Origin of metazoan cadherin diversity and the antiquity of the classical cadherin/β-catenin complex. Proc. Natl. Acad. Sci. USA 109, 13046–13051.
Oda, H., Tsukita, S., Takeichi, M., 1998. Dynamic behavior of the cadherin-based cell–cell adhesion system during drosophila gastrulation. Dev. Biol. 203, 435–450.
Park, C., Falls, W., Finger, J.H., Longo-Guess, C.M., Ackerman, S.L., 2002. Deletion in Catna2, encoding alpha N-catenin, causes cerebellar and hippocampal lamination defects and impaired startle modulation. Nat. Genet 31, 279–284.
Peng, X., Cuff, L.E., Lawton, C.D., DeMali, K.A., 2010. Vinculin regulates cell-surface E-cadherin expression by binding to beta-catenin. J. Cell Sci. 123, 567–577.
Plotnikov, S.V., Pasapera, A.M., Sabass, B., Waterman, C.M., 2012. Force fluctuations within focal adhesions mediate ECM-rigidity sensing to guide directed cell migration. Cell 151, 1513–1527.
Pukhlyakova, E., Aman, A.J., Elsayad, K., Technau, U., 2018. β-catenin–dependent mechanotransduction dates back to the common ancestor of Cnidaria and Bilateria. Proc. Natl. Acad. Sci..
Ragkousi, K., Marr, K., McKinney, S., Ellington, L., Gibson, M.C., 2017. Cell-cycle-coupled oscillations in apical polarity and intercellular contact maintain order in embryonic epithelia. Curr. Biol. 27, 1381–1386.
Rentzsch, F., Fritzenwanker, J.H., Scholz, C.B., Technau, U., 2008. FGF signalling controls formation of the apical sensory organ in the cnidarian Nematostella vectensis. Development 135, 1761–1769.
Rimm, D.L., Koslov, E.R., Kebriaei, P., Cianci, C.D., Morrow, J.S., 1995. Alpha 1(*E*)-catenin is an actin-binding and -bundling protein mediating the attachment of F-actin to the membrane adhesion complex. Proc. Natl. Acad. Sci. USA 92, 8813–8817.
Röttinger, E., Dahlin, P., Martindale, M.Q., 2012. A framework for the establishment of a cnidarian gene regulatory network for "endomesoderm" specification: the inputs of ß-catenin/TCF signaling. PLoS Genet. 8, e1003164.
Ryan, J.F., Mazza, M.E., Pang, K., Matus, D.Q., Baxevanis, A.D., Martindale, M.Q., Finnerty, J.R., 2007. Pre-bilaterian origins of the Hox cluster and the Hox code: evidence from the sea anemone, Nematostella vectensis. PloS One 2, e153.
Salinas-Saavedra, M., Rock, A.Q., Martindale, M.Q., 2018. Germ layer-specific regulation of cell polarity and adhesion gives insight into the evolution of mesoderm. eLife 7,

e36740.
Sarpal, R., Pellikka, M., Patel, R.R., Hui, F.Y.W., Godt, D., Tepass, U., 2012. Mutational analysis supports a core role for Drosophila α-catenin in adherens junction function. J. Cell Sci. 125, 233–245.
Schippers, K.J., Nichols, S.A., 2018. Evidence of signaling and adhesion roles for β-catenin in the sponge ephydatia muelleri. Mol. Biol. Evol. 35, 1407–1421.
Sebé-Pedrós, A., Irimia, M., del Campo, J., Parra-Acero, H., Russ, C., Nusbaum, C., Blencowe, B.J., Ruiz-Trillo, I., 2013. Regulated aggregative multicellularity in a close unicellular relative of metazoa. eLife 2, e01287.
Sinigaglia, C., Busengdal, H., Leclere, L., Technau, U., Rentzsch, F., 2013. The bilaterian head patterning gene six3/6 controls aboral domain development in a cnidarian. PLoS Biol. 11, e1001488.
Srivastava, M., Simakov, O., Chapman, J., Fahey, B., Gauthier, M.E., Mitros, T., Richards, G.S., Conaco, C., Dacre, M., Hellsten, U., 2010. The Amphimedon queenslandica genome and the evolution of animal complexity. Nature 466, 720–726.
Steinmetz, P.R., Aman, A., Kraus, J.E., Technau, U., 2017. Gut-like ectodermal tissue in a sea anemone challenges germ layer homology. Nat. Ecol. Evol. 1, 1535.
Stepniak, E., Radice, G.L., Vasioukhin, V., 2009. Adhesive and signaling functions of cadherins and catenins in vertebrate development. Cold Spring Harb. Perspect. Biol., 1.
Takeichi, M., 1977. Functional correlation between cell adhesive properties and some cell surface proteins. J. Cell Biol. 75, 464–474.
Takeichi, M., 1988. The cadherins: cell-cell adhesion molecules controlling animal morphogenesis. Development 102, 639–655.
Torres, M., Stoykova, A., Huber, O., Chowdhury, K., Bonaldo, P., Mansouri, A., Butz, S., Kemler, R., Gruss, P., 1997. An alpha-E-catenin gene trap mutation defines its function in preimplantation development. Proc. Natl. Acad. Sci. USA 94, 901–906.
Townes, P.L., Holtfreter, J., 1955. Directed movements and selective adhesion of embryonic amphibian cells. J. Exp. Zool. Part A: Ecol. Genet. Physiol. 128, 53–120.
Tulin, S., Aguiar, D., Istrail, S., Smith, J., 2013. A quantitative reference transcriptome for Nematostella vectensis early embryonic development: a pipeline for de novo assembly in emerging model systems. Evodevo 4, (16-16).
Uchida, N., Shimamura, K., Miyatani, S., Copeland, N.G., Gilbert, D.J., Jenkins, N.A., Takeichi, M., 1994. Mouse alpha N-catenin: two isoforms, specific expression in the nervous system, and chromosomal localization of the gene. Dev. Biol. 163, 75–85.
Varner, J.A., 1995. Cell adhesion in sponges: potentiation by a cell surface 68 kDa proteoglycan-binding protein. J. Cell Sci. 108, 3119–3126.
Wijesena, N., Simmons, D.K., Martindale, M.Q., 2017. Antagonistic BMP–cWNT signaling in the cnidarian *Nematostella vectensis* reveals insight into the evolution of mesoderm. Proc. Natl. Acad. Sci..
Wikramanayake, A.H., Hong, M., Lee, P.N., Pang, K., Byrum, C.A., Bince, J.M., Xu, R., Martindale, M.Q., 2003. An ancient role for nuclear beta-catenin in the evolution of axial polarity and germ layer segregation. Nature 426, 446–450.
Wilson, H., 1907. On some phenomena of coalescence and regeneration in sponges. J. Exp. Zool. 5, 245–258.
Wolenski, F.S., Layden, M.J., Martindale, M.Q., Gilmore, T.D., Finnerty, J.R., 2013. Characterizing the spatiotemporal expression of RNAs and proteins in the starlet sea anemone, Nematostella vectensis. Nat. Protoc. 8, 900–915.